Int J Clin Exp Pathol 2016;9(3):2960-2969
www.ijcep.com /ISSN:1936-2625/IJCEP0020186

Original Article

The role of CD40 and CD40L in the pathogenesis of an experimental model of choroidal neovascularization

Fang Liu[1], Peipei Zhang[2], Kesheng Wang[1], Fang Wang[1], Jianming Zhi[3]

[1]Department of Ophthalmology, Shanghai Tenth People's Hospital of Tongji University, Shanghai, China; [2]Wenzhou Ophthalmology and Optometry Hospital, Wenzhou Medical University, Wenzhou, Zhejiang, China; [3]Department of Physiology, School of Medicine, Shanghai Jiaotong University, Shanghai, China

Received November 20, 2015; Accepted February 15, 2016; Epub March 1, 2016; Published March 15, 2016

Abstract: Objective: To evaluate the effect of intravitreal injection with anti-CD40 ligand antibody (anti-CD40L) on choroidal neovascularization (CNV) in a laser-induced CNV mouse model. Methods: Anti-CD40L (0.5 mg/ml, 1 μl), anti-VEGF (0.5 mg/ml, 1 μl) or PBS (1×, 1 μl) was injected into the vitreous body of C57BL/6J mice at day 3 after laser photocoagulation. Changes in CNV lesions were evaluated by immunofluorescence staining and immunohistochemistry of the CNV sites in retinal pigment epithelium (RPE)-choroid-sclera flat mounts. Expression of VEGF was detected by real-time quantitative PCR (RT-PCR) to explore the inhibitory effect of anti-CD40L on CNV progression. Results: Compared with the CNV model group, anti-CD40L group and anti-VEGF group showed significant regression of the experimental CNV as represented by a 42.87% and 50.87% reduction of the hyper-fluorescence area of the CNV lesion, respectively (both $P<0.01$). Histological images shows that the CNV lesions in anti-CD40L group were smaller in diameter and had thinner centers compared with those in the control group. Immunohistochemistry showed that the expression level of VEGF-A was suppressed after up-regulation of CD40L. Real Time-PCR analysis showed that the expression of VEGF in the photocoagulated choroid tissue was reduced after blocking CD40L. Conclusion: Anti-CD40L effectively inhibited CNV in the experimental laser-induced CNV model, suggesting that anti-CD40L may prove to be a clue for the treatment of CNV.

Keywords: CD40 ligand, anti-CD40L antibody, vascular endothelial growth factor (VEGF), choroidal neovascularization

Introduction

Choroidal neovascularization (CNV) is known to be the result of outgrowth of new blood vessels from the choriocapillaries and penetration through the Bruch membrane into the subretinal pigment epithelial or subretinal space. CNV can be induced in multiple diseases including age-related macular degeneration (AMD), pathologic myopia and ocular trauma. Although there have been many experiments to explore the causes of CNV, the exact pathogenesis of CNV formation and development remains to be fully elucidated. Vascular endothelial growth factor (VEGF) as a major proangiogenic factors is believed to be involved in the pathogenesis of CNV [1, 2]. However, investigations on non-VEGF components that are involved in the development of CNV have been reported.

Interactions between CD40 and CD40L is known to promote activation of T and B cells and maturation of myeloid-derived antigen presenting cells (APCs), thus facilitating immune responses [3-6]. Dysregulation in the CD40-CD40L co-stimulation pathway is featured prominently in systemic autoimmune and tissue-specific autoimmune diseases [7-10]. CD40L level is positively correlated with hepatic immunoglobulin (Ig) production [11]. Sheetal et al [12] reported that the double-stranded RNA-dependent protein kinase (PKR) played a critical role in Ig expression as a novel downstream effector molecule for CD40 signaling [12]. Many observations have defined CD40L-CD40 interactions to be crucial for adaptive immune responses [13-15].

Nevertheless, beyond its function on immune cells, CD40-induced responses have also been found to mediate angiogenesis [16-19]. Dormond et al [20] concluded that CD40-CD40L interactions and the associated expression of VEGF represented a mechanistic link

between immunity and the development of angiogenesis in endothelial cells.

Although CD40-CD40L is known to be involved in the formation of neovascular tissue in other organs, whether CD40-CD40L is involved in the development of CNV and whether the lack of CD40-CD40L or the administration of anti-CD40L can inhibit the development of experimental CNV remain to be determined. In the present study, we investigated the anti-angiogenic effect of anti-CD40L on experimental laser-induced CNV in mice, in an attempt to see whether VEGF up-regulation is preceded by anti-CD40L and whether anti-CD40L may serve as a target for earlier and potentially protective intervention.

Materials and methods

Antibodies and reagents

Anti-CD40L and anti-VEGF (Abcam, Cambridge, MA, USA) were stored at -20°C and thawed immediately prior to administration to mice.

Animals

C57BL/6J strain background male mice aged 4-6 weeks weighing 20-22 g (Animal facilities of the 10th People's Hospital of Tongji University, Shanghai, China) were fed a normal diet and maintained in individually ventilated cages under specific pathogen-free conditions. All protocols were reviewed and approved by the Institutional Animal Case and Use Committee of Tongji University School of Medicine (Shanghai, China). The animals were treated according to the guidelines of the ARVO Statement for the Use of Animals in Ophthalmic Research.

Laser-irradiated CNV in mice

Forty mice were equally randomized to four groups: 1) control group; 2) CNV model group (CNV model + intravitreal injection (IVT) of PBS (1×, 1 μl); 3) anti-CD40L group (CNV model + IVT anti-CD40L VEGF (0.5 mg/ml, 1 μl); and 4) anti-VEGF group (CNV model + IVT anti-VEGF (0.5 mg/ml, 1 μl)). All treatments were performed at day 3 after laser photocoagulation, and all injections were performed by using a Hamilton microinjector.

Establishment of the CNV model

After general anesthesia with pentobarbital (50 mg/kg, ip), the mouse pupils were dilated with compound tropicamide eye drops (Mydrin-P, Santen). After superficial anesthesia with 0.5% proparacaine hydrochloride (Alcaine, Alcon), laser photocoagulation-induced rupture of Bruch's membrane was performed on the right eye under slit lamp microscope observation and the argon laser photocoagulator using the following laser parameters: 100 μm spot size, 200 mW intensity, and 0.1 s duration. A cover slip was applied to the cornea to view the retina with sodium hyaluronate. Six lesions were produced within two or three disc diameters of the optic disc. Only mice that experienced a cavitation bubble indicating a rupture in the Bruch's membrane without hemorrhage in the ocular fundus were included in the study. Finally, 40 laser-irritated CNV mice were used.

Fluorescein angiography

Fluorescein angiography was performed with a fundus camera (Heidelberg Spectralis HRA, Germany). At 1 week after laser photocoagulation and intraperitoneal (ip) injection of 0.1 mL 1% fluorescein sodium (Alcon, Tokyo, Japan), photographs were captured with a 20-D lens in contact with the fundus camera lens. The fluorescein angiograms were evaluated by a retina specialist who was blind to the laser therapy. Lesions were graded on an ordinal scale based on the spatial and temporal evolution of fluorescein leakage as follows: 0 (nonleaky) no leakage, faint hyperfluorescence, or mottled fluorescence without leakage; 1 (questionable leakage) hyperfluorescent lesion without progressive increase in size or intensity; 2 (leaky) hyperfluorescence increasing in intensity but not in size, no definite leakage; 3 (pathologically significant leakage) hyperfluorescence increasing in intensity and in size, definite leakage (**Figure 1**).

Measurement of CNV lesions by immunofluorescence staining

Two weeks after laser injury, the mice were euthanized, and their eyes were fixed in eye special stationary liquid (Eye & Ent of Fudan University) for 30 min. The immunofluorescence staining techniques were used to label endothelial cells within CNV lesions; the cor-

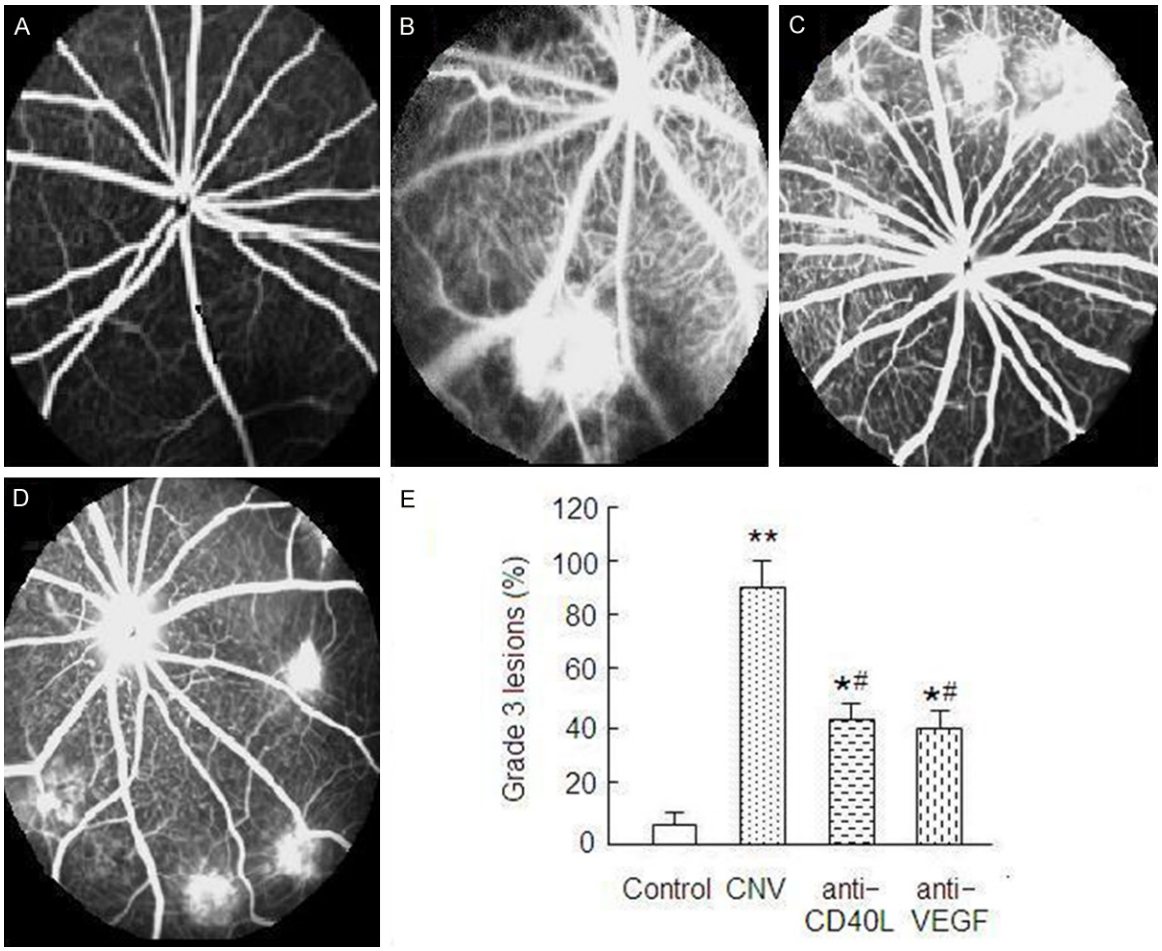

Figure 1. Pathologically significant leakage (grade 3 lesions) was observed mostly in the CNV model group, and rarely seen in the anti-CD40L and anti-VEGF groups. A: Control group; B: CNV model group; C: Anti-VEGF group; D: Anti-CD40L group; E: Percentages of grade 3 lesions. *P<0.001 *vs.* control group; #P<0.01 *vs.* CNV model group.

nea, iris, lens and vitreous body were removed from the sclera, and the retinal neuroepithelium was gently peeled and separated from the underlying retinal pigment epithelium (RPE) to obtain the RPE-choroid-sclera eyecup. After four radial incisions were made from the edge to the equator, the RPE-choroid-sclera eyecup was flat-mounted, and the remaining eyecups were rinsed in the blocking solution containing 10% normal donkey serum and 0.1% polysorbate 20 (Tween20, Sigma) diluted in PBS, and then incubated with a 1:100 dilution of CD31 overnight at 4°C. The secondary antibody was 1:100 dilution of Alexa Fluor 488 (Abcam). Finally, the eye cups were washed with cold PBS, flat-mounted and glass-covered with the RPE eye side facing up. The images were digitalized by scanning laser confocal microscopy (Zeiss) and Image J software was used to evaluate the size of the hyper-fluorescent areas corresponding to CNV.

CNV histopathology

Each of three laser-induced CNV mice in all groups were used for histological and immunohistochemical evaluation. Fourteen days after laser photocoagulation, the mice were euthanized. The cornea, lens and vitreous body fixed in eye special stationary liquid were removed from enucleated eyes. The eyes were paraffin embedded, sliced into 4-μm sections throughout the entire extent of laser burn, and stained with haematoxylin and eosin (HE).

CNV immunohistochemistry

Immunohistochemical staining with anti-VEGFA factor was performed according to the manu-

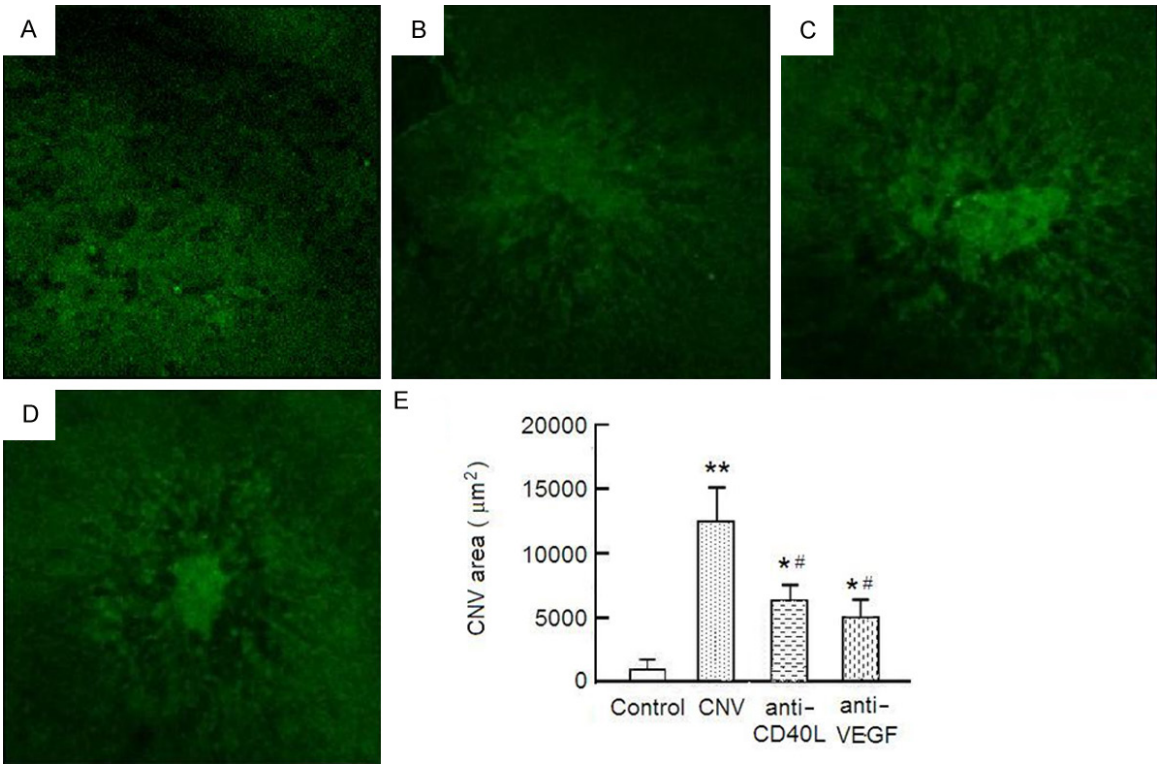

Figure 2. Immunofluorescence staining of choroidal neovascularization (CNV) lesions in RPE-choroid-sclera flat mounts was obtained 14 days after laser photocoagulation. A: Control group; B: CNV model group; C: Anti-VEGF group; D: Anti-CD40L group; E: The areas of CNV lesions in the 4 groups. *P<0.001 *vs.* control group; #P<0.01 *vs.* CNV model group.

facturer's protocol using the EnVison (ELPS, Enhance Labeled Polymer System) method (Dako). Briefly, sections were deparaffinized and then treated with 3% hydrogen peroxide to block endogenous peroxidase activity. After washing with PBS (0.01 mmol/L; pH 7.4), the sections were incubated with anti-VEGF overnight at 4°C, rinsed with PBS, and then treated with DAB at room temperature. For transmission electron microscopy, the eyes were fixed as described above, post-fixed in hematoxylin, and dehydrated in ethanol. After substitution with xylene, the specimens were embedded in Epoxy resin. These sections (1/Ltm) were stained with 0.05% toluidine blue in 0.1 M phosphate buffer (pH 7.4). Ultrathin sections were examined with a Nikon Eclipse 50i and analyzed using Image pro plus 6.0 software. The images were taken at 200 magnification.

Real-time polymerase chain reaction (RT-PCR) analysis

The eyes were collected on day 14 after immunization for RNA purification. The tissue was snap frozen in liquid nitrogen within 30 s of collection, stored at -80°C before being homogenized (Power Gen 35 homogenizer; Fisher Scientific) in 1 ml Trizol reagent (Invitrogen), incubated on ice for 15 min, and extracted with 200 μl chloroform for 5 min. Samples were then precipitated with isopropanol and washed with 75% ethanol. RNA (0.5 mg) was converted to cDNA using commercially available gene primers and probes (Bogu Biochemics) with PrimeScript RT-PCR kit and Premix EX Taq (TaKaRa) according to manufacturer's instruction. Individual sample cDNA (50 ng) was used as a template for real-time PCR. The reaction mixtures were subjected to the following amplification: denaturing at 95°C for 30 s, followed by 50 cycles of melting at 95°C for 5 s, annealing at 60°C for 31 s. Real-time PCR data were analyzed using Sequence Detector version 1.7.1 software included with the 7700 Sequence Detector Systems (Applied Biosystems). All data were normalized to the endogenous reference gene glyceraldehyde-3-phosphate dehydrogenase (GAPDH). All data were checked for homogeneity by dissociation curve analysis. Fluorescence changes were monitored after each cycle, and Ct (threshold cycle) values for amplification of CD40, VEGF

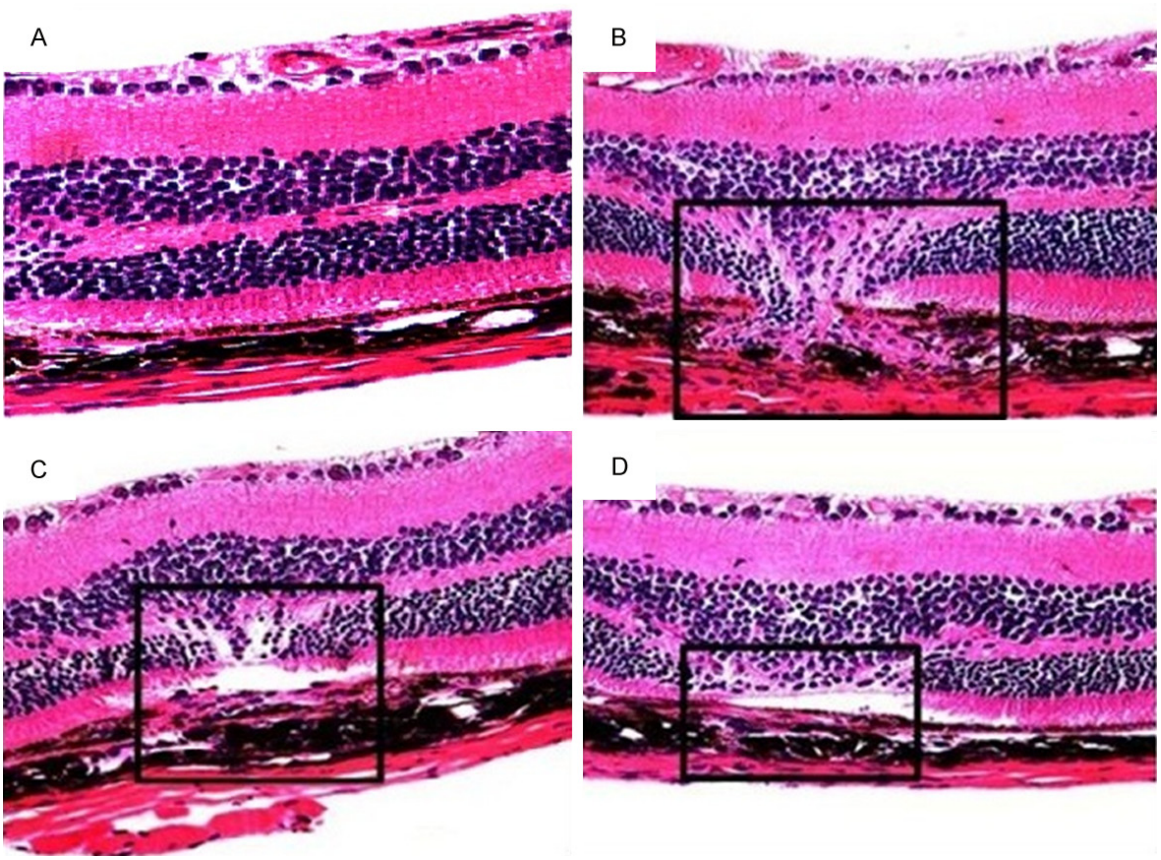

Figure 3. Histology of choroidal neovascularization (CNV) lesions stained with hematoxylin-eosin was obtained 14 days after laser photocoagulation. Dome-like CNV complexes, consisting of fibrovascular tissue, retinal epithelial cells and pigment clumps, are shown in the control group (A), CNV model group (B), anti-VEGF group (C), and anti-CD40L group (D). The outgrowth of CNV lesions in the group receiving intravitreal injections of anti-CD40L antibody was smaller in size and had a thinner center compared with the baseline and P CNV model group. Scale bar, 100 μm.

and endogenous of glyceraldehyde-3-phosphate dehydrogenase (GAPDH) mRNA were defined.

Statistical analysis

A left spherically distributed (LSD) test was used for statistical analyses of the areas of the CNV lesions obtained by immunofluorescence staining using SPSS (SPSS version 17.0). The outcomes of RT-PCR were statistically analyzed with the LSD test. Results were expressed as mean ± standard deviation, and column chart. *P* values <0.05 were considered statistically significant.

Results

Angiograms in laser-induced CNV mice

At 1 week after laser photocoagulation, pathologically significant leakage (grade 3 lesions) was observed in most animals of the CNV model group but rarely seen in the anti-CD40L and anti-VEGF groups (both P<0.01). There was no significant difference in leakage between the anti-CD40L and anti-VEGF groups (**Figure 1**).

Quantitation of CNV lesions by immunofluorescence staining

Images of the CNV lesions in RPE-choroid-sclera flat-mount showed representative from CNV, anti-CD40L and anti-VEGF on day 14 after laser injury (**Figure 2**). Quantification of CNV lesions from the three groups are summarized in **Figure 2E**. The area of CNV model group was 11990 ± 2541 μm^2. There was no statistically significant difference between the anti-VEGF group and anti-CD40L group (6164 ± 1635 μm^2 *vs.* 5195 ± 1729 μm^2, P>0.05). But the

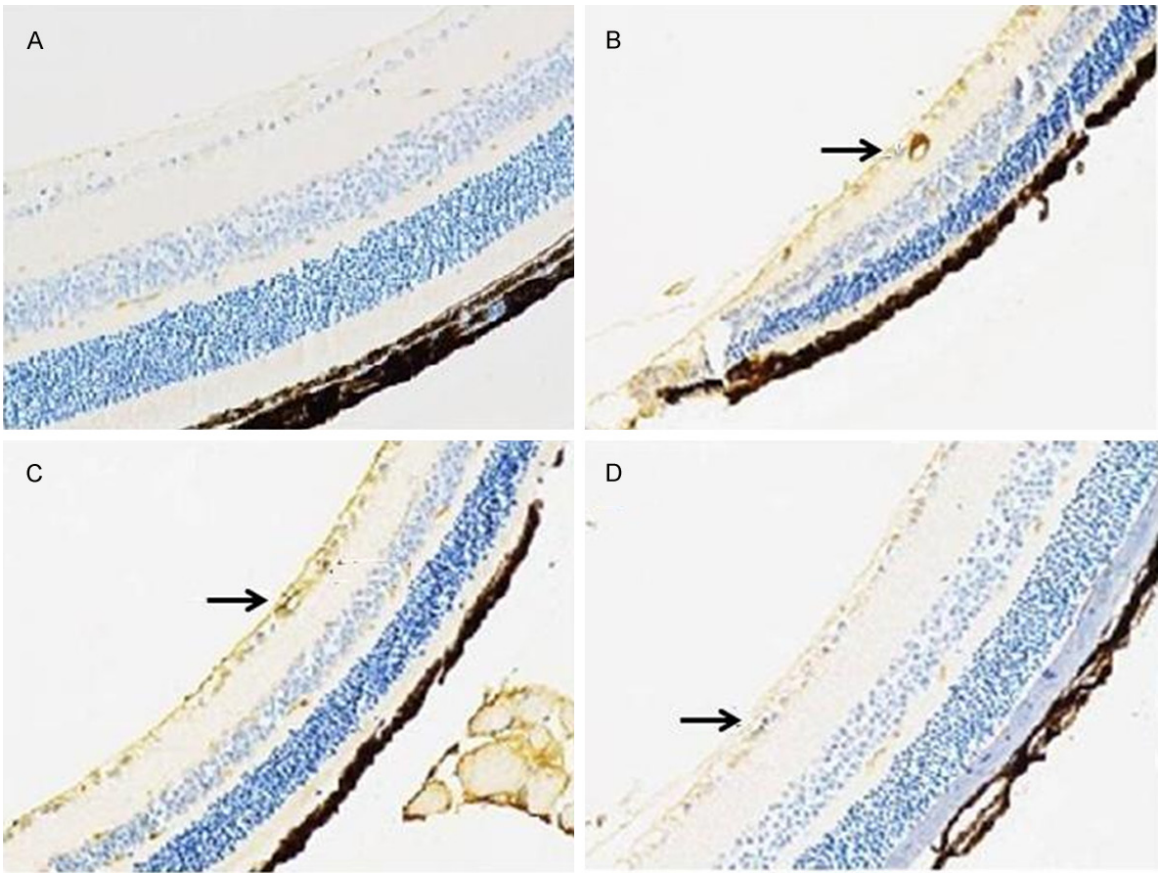

Figure 4. Immunohistochemical staining of CD40L 14 days after photocoagulation (200 ×). A: Control group; B: CNV model group; C: Anti-VEGF group; D: Anti-CD40L. A large number of yellow particles were widely distributed in the outer layer, inner core, inner plexus and cell layer; CD40L was highly expressed in B and C. Few yellow particles were seen distributing in the outer layer, inner core and cell layer in A. Low expression of CD40L was observed in D.

analysis of the hyper-fluorescent area according to CNV sites revealed that the area of CNV lesions in the anti-CD40L and anti-VEGF groups was significantly smaller than that in the CNV model group (both $P<0.001$), indicating that the established CNV regressed in the anti-CD40L group. After intravitreal injection with anti-CD40L and anti-VEGF, the area of CNV lesions was reduced by 42.87% and 50.87% respectively as compared with the CNV model group.

Histologic assessment of CNV

Histological retinal sections were analyzed on day 14 after laser treatment using HE staining. There was a discontinuity in the Bruch membrane in the area of each laser burn in both control and treatment groups. At the site of laser spots, the area of fibrovascular tissue consisting of a vascular lumen was observed. The CNV complexes consisting of fibrovascular tissue, RPE and pigment clups emerged through the ruptured Bruch's membrane, demonstrating that CNV lesions in the anti-CD40LAb and anti-VEGF treated mice were smaller in diameter and had thinner centers compared with those in the CNV model group (**Figure 3**). Measurement of the relative thickness of the CNV membrane in the lesions showed differences in the extent of CNV. The size of the outgrowth of CNV lesions in the anti-CD40L antibody group was smaller with a thinner center as compared with that in the CNV model group.

Expression pattern of VEGF in laser-irradiated choroidal tissue

VEGF protein was readily observed immunohistochemically in the laser-injured cells of the choroidal tissue. We then examined whether such upregulation of CD40L might affect the expression level of VEGFA by injecting IVT with anti-CD40L neutralization antibody. It was found that blocking CD40L by intravitreal injec-

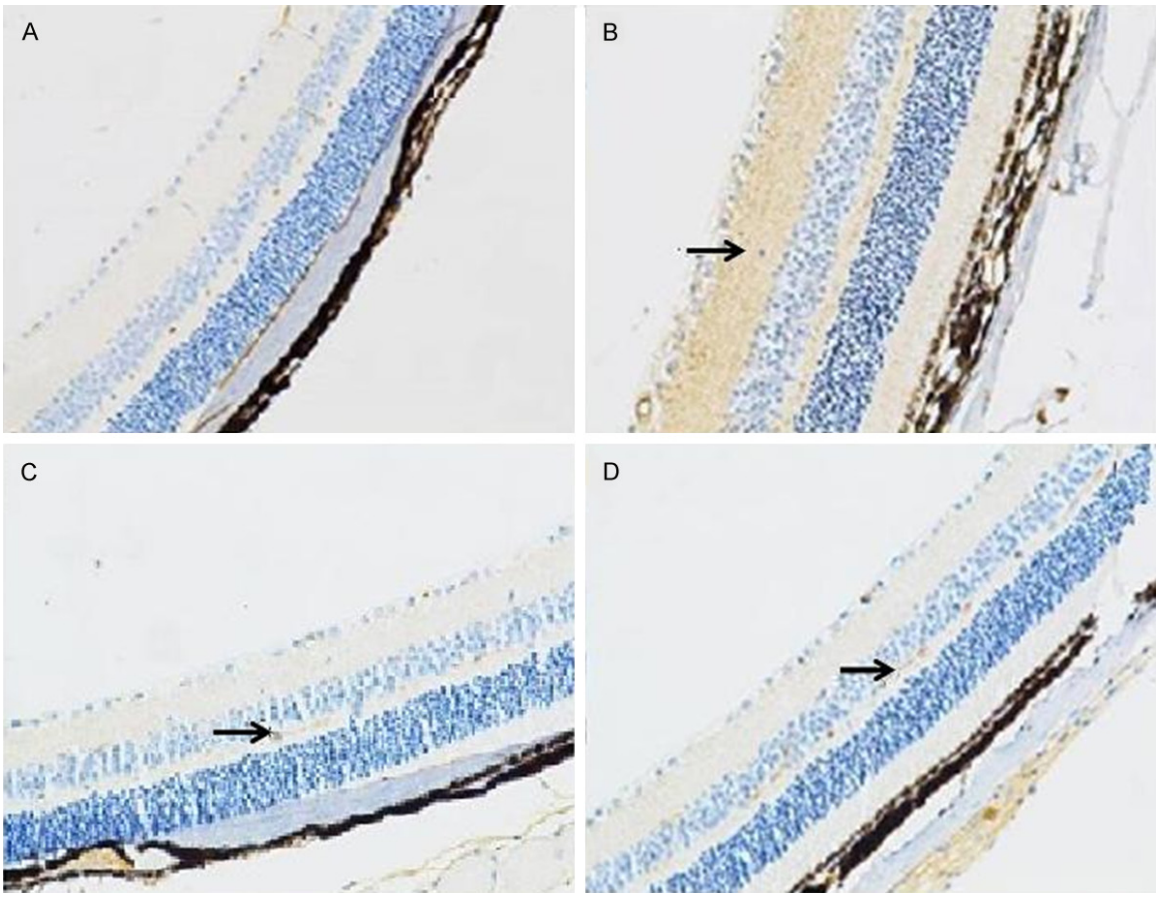

Figure 5. Immunohistochemical staining of VEGF-A 14 days after photocoagulation (200 ×). A: Control group; B: CNV model group; C: Anti-VEGF group; D: Anti-CD40L group. A large number of yellow particles were widely distributed in the outer layer, inner core, inner plexus and cell layer. VEGF-A was highly expressed in B. Few yellow particles were seen distributing in the outer layer, inner core and cell layer in A. Low expression of VEGF-A was observed in D.

tion of the neutralization antibody inhibited VEGF expression.

To observe the successful inhibition of CNV with CD40L after injection of anti-CD40L, the pathological blank sections of each group were examined by CD40L immunohistochemical staining at day 14 after photocoagulation. The yellow or brown yellow particles under the microscope indicate positive expressions, and the blue color indicates the nucleus. No CD40L expression was observed in the mouse normal tissues (**Figure 4**). In the CNV model group and anti-VEGF group, a large number of yellow particles were seen distributing in the outer layer, inner core, inner plexus and cell layer. In the anti-CD40L group, only a few yellow particles were seen in the outer layer, inner core layer and cell layer. The amount of CD40L expression was significantly less than that in the CNV model group and anti-VEGF group.

To see whether the inhibition of CNV with VEGF was successful, the pathological blank sections of each group were examined by VEGF-A immunohistochemical staining at day 14 after photocoagulation. The yellow or brown yellow particles indicate positive expressions, and the blue color indicates the nucleus. As shown in **Figure 5**, the VEGF expression was low in the normal tissues. In the CNV model group, a large number of yellow particles were seen distributing in the outer layer, inner core, inner plexus and cell layer, while in the anti-CD40L group and VEGF group, only a few yellow particles were seen in these locations. The amount of VEGF expression was significantly less than that in the CNV model group.

Regression of established CNV after treatment by RT-PCR analysis

Real-time-PCR analysis showed that the expression of VEGF in the photocoagulated choroidal

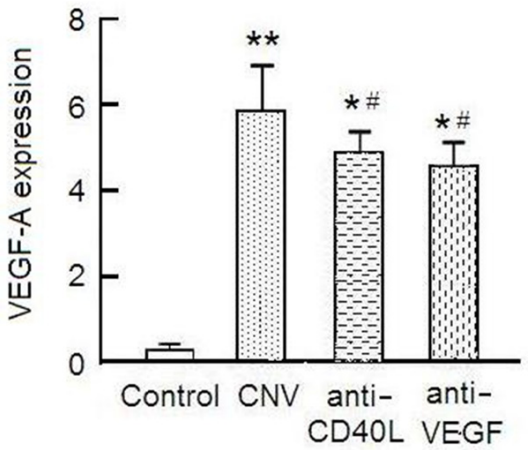

Figure 6. The expression of mRNA VEGF after 14 days. mRNA VEGF was detected by QPCR. There was no significant difference in the expression of mRNA VEGF between the anti-VEGF group and the anti-CD40L group ($P>0.05$). However, the expression of mRNA VEGF in the anti -VEGF and anti-CD40L groups was lower than that in the CNV model group. $^{*}P<0.001$ *vs.* control group; $^{\#}P<0.01$ *vs.* CNV model group.

tissue was suppressed after blocking CD40L. Real Time-PCR showed that VEGF-A expression in RPE/choroid of anti-CD40 eye was significantly depressed ($P<0.01$) compared with the CNV group. These results prompted us to hypothesize that the growth of experimental CNV could be probably affected by blocking CD40L (**Figure 6**).

Discussion

Patients with CNV-associated visual impairment are currently managed with anti-VEGF therapies. A number of recent clinical trials have demonstrated that successful CNV growth arrest can help maintain or improve visual acuity following VEGF inhibition [1]. However, many patients still experienced deteriorating vision and disease progression despite these treatments. Thus, new selective antiangiogenic drugs are highly desirable for potential complications in patients with persistent recurrent CNV and other ocular pathologic neovascularizations.

Previous studies [21] showed that infiltrating macrophages played a critical role in laser-induced CNV. Melter et al [16] demonstrated that the interaction between T cells and macrophages via CD40/CD40L had a potent effect on VEGF expression, which may further cause VEGF-induced angiogenesis.

Given the role of CD40 in immune response, CD 40/CD40L binding can induce activation and proliferation of lymphocytes, mononuclear cells, macrophages and other inflammatory cells. Activated lymphocytes and monocytes and macrophages could secrete a large number of cytokines including VEGF angiogenic factor, suggesting that CD40 is capable of regulating the role of angiogenesis. Dormond et al [20] found that the activation of VEGF was regulated by inhibition of sCD40L.

In our experiment, we evaluated the role of CD40 in angiogenesis in a murine laser-induced CNV model, and used several methods to measure CNV to reinforce our finding. We examined the level of angiogenic gene expression after blocking CD40L. Real-time qPCR showed the expression of VEGF in the healing choroidal tissue after laser irradiation was suppressed after intravitreal injection of anti-CD40L. Additionally, immunfluorescence analysis showed that the mean hyper-fluorescent area according to the laser-induced CNV lesions decreased by 50.87% in the group injected with anti-CD40L compared with the CNV group. All these findings indicate that anti-CD40L could inhibit laser-induced angiogenesis and the associated expression of VEGF in vivo. These findings further prompted us to hypothesize that CD40-CD40L might be involved in the development of laser-induced experimental CNV in mice.

CD40 is a newly identified pathway contributing to ocular pathological angiogenesis such as CNV [21]. In agreement with their report, our study showed that CNV suppression by the CD40 antagonist was independent of the total VEGF expression, and that the CD40 antagonist suppressed eotaxin expression after laser injury.

Some published studies [16-19] reported that lacking or blocking CD40-CD40L could inhibit the occurrence of angiogenesis. A study [22] showed that sCD40L could inhibit gastric cancer growth, and halt tumor cell invasion and transfer via activating CD40 signal. Moreover, CD40L blockade has been shown to inhibit angiogenesis and slow down the growth of breast tumors [18, 19]. As for nonneoplastic tissues, CD40L is reportedly involved in tissue

immune activity in various tissues. It was reported [23] that administration of sCD40L had a therapeutic effect on several chronic immune inflammatory diseases including arthritis, inflammatory bowel disease, asthma, and chronic allograft rejection. It was found in these experimental disease models that blocking CD40-CD40L activity could suppress pathologic angiogenesis.

In addition to the CD40-CD40L effect on local tissue inflammation and subsequent local expression level of anti-angiogenic cytokines, CD40/CD40L could reportedly affect the behavior of vascular endothelial cells. The effect of CD40L on in vitro neovascularization by cultured vascular endothelial cells and cell signaling were investigated. Dormond et al [20] found that the injection of CD40L transfectants resulted in VEGF expression and mediated a marked angiogenesis reaction through mTORC2 and Akt pathway. Additionally, Ramello et al [24] found that blocking mAbs against CD40 ligand reduced the production of pro-inflammatory cytokines and angiogenic factors. Blockade of CD40L/CD40 interaction reduced the production of IL-1β, IL-6, TNF and IL-8. It was found that after anti-CD40L treatment, the amount of VEGF-A was reduced in most CCs from different donors [24].

In the present study, we explored the effect of local blockade of CD40-CD40L co-stimulation on the outcome of experimental CNV. The results showed that local, rather than systemic, blockade of the CD40/CD40L co-stimulatory pathway could at least in part modulate the immune response generated to choroidal neovascularization. However, the mechanism underlying this effect in the target site remains to be elucidated.

In summary, our data provide evidence that endogenous CD40L at physiological level could inhibit experimental angiogenesis in laser-induced CNV in vivo. The action mechanism might include the effect of CD40L on vascular endothelial cells. Blocking CD40L activity might be a potential strategy for the prevention or treatment of CNV-related diseases. All our findings indicate that anti-CD40 ligand antibody has a beneficial effect in the treatment of experimental CNV. Further studies on the therapeutic mechanism of action are required to determine the applicability of anti-CD40L for the treatment of CNV.

Disclosure of conflict of interest

None.

Address correspondence to: Dr. Fang Liu, Department of Ophthalmology, Shanghai Tenth People's Hospital of Tongji University, 301 Yanchang Rd, Shanghai 200072, China. Tel: +86 21 66301542; Fax: +86 21 66301542; E-mail: fangliu_2004@yahoo.com; Jianming Zhi, Department of Physiology, School of Medicine, Shanghai Jiaotong University, 280 South Chongqing Road, Shanghai 200025, China. Tel: +86 21 66301542; Fax: +86 21 66301542; E-mail: zhjm169@gmail.com

References

[1] Krause TA, Alex AF, Engel DR, Kurts C, Eter N. VEGF-Production by CCR2-Dependent Macrophages Contributes to Laser-Induced Choroidal Neovascularization. PLoS One 2014; 9: e94313.

[2] Matri L, Chebil A, Kort F. Current and emerging treatment options for myopic choroidal neovascularization. Clin Ophthalmol 2015; 9: 733-744.

[3] Danese S, Sans M, Fiocchi C. The CD40/CD40L costimulatory pathway in inflammatory bowel disease. Gut 2004; 53: 1035-1043.

[4] Richer MJ, Lavallléee DJ, Shanina I, Horwitz MS. Immunomodulation of Antigen Presenting Cells Promotes Natural Regulatory T Cells That Prevent Autoimmune Diabetes in NOD Mice. PLoS One 2012; 7: e31153.

[5] Brunekreeft KL, Strohm C, Gooden MJ, Rybczynska AA, Nijman HW, Grigoleit GU, Helfrich W, Bremer E, Siegmund D, Wajant H, de Bruyn M. Targeted delivery of CD40L promotes restricted activation of antigen-presenting cells and induction of cancer cell death. Mol Cancer 2014; 13: 85.

[6] Elmetwali T, Young LS, Palmer DH. Fas-associated factor (Faf1) is a novel CD40 interactor that regulates CD40-induced NF-κB activation via a negative feedback loop. Cell Death Dis 2014; 5: e1213.

[7] Ciferska H, Horák P, Heřmanová Z, Ordeltováet M, Zadražil J, Tichý T, Scudla V. The levels of sCD30 and of sCD40L in a group of patients with systemic lupus erythematodes and their diagnostic value. Clin Rheumatol 2007; 26: 723-8.

[8] Tanaka H, Yang GX, Iwakoshi N, Knechtle SJ, Kawata K, Leung P, Coppel RL, Ansari AA, Joh T, Bowlus C, Gershwin ME. Anti-CD40 ligand

monoclonal antibody delays the progression of murine autoimmune cholangitis. Clin Exp Immunol 2013; 174: 364-371.
[9] Vinay DS, Kwon BS. The tumour necrosis factor/TNF receptor superfamily: therapeutic targets in autoimmune diseases. Clin Exp Immunol 2011; 164: 145-157.
[10] Ludwiczek O, Kaser A, Tilg H. Plasma levels of soluble CD40 ligand are elevated in inflammatory bowel diseases. Int J Colorectal Dis 2003; 18: 142-147.
[11] Mayo MJ, Mosby JM, Jeyarajah R, Combes B, Khilnani S, Al-halimi M, Handem I, Grammer AC, Lipsky PE. The relationship between hepatic immunoglobulin production and CD154 expression in chronic liver diseases. Liver Int 2006; 26: 187-96.
[12] Thakur SA, Zalinger ZB, Johnson TR, Imani F. Protein Kinase R Is a Novel Mediator of CD40 Signaling and Plays a Critical Role in Modulating Immunoglobulin Expression during Respiratory Syncytial Virus Infection. Clin Vaccine Immunol 2011; 18: 2060-2066.
[13] Bremer E. Targeting of the Tumor Necrosis Factor Receptor Superfamily for Cancer Immunotherapy. Oncol 2013; 2013: 371854.
[14] Bakdash G, Sittig SP, van Dijk T, Figdor CG, de Vries IJ. The nature of activatory and tolerogenic dendritic cell-derived signal II. Front Immunol 2013; 4: 53.
[15] Peters AL, Stunz LL, Bishop GA. CD40 and autoimmunity: the dark side of a great activator. Semin Immunol 2009; 21: 293-300.
[16] Hristov M, Gumbel D, Lutgens E, Zernecke A, Weber C. Soluble CD40 ligand impairs the function of peripheral blood angiogenic outgrowth cells and increases neointimal formation after arterial injury. Circulation 2010; 121: 315-324.
[17] Zhang PP, Su Y, Liu F. The relationship between intervention in the CD40 signal pathway and choroidal neovascularization. Oncol Targets Ther 2014; 7: 263-267.
[18] Vornhagen AS, Draube A, Liebig TM, Rothe A, Kochanek M, Baildon MS. The immunosuppressive factors IL-10, TGF-β, and VEGF do not affect the antigen-presenting function of CD40-activated B cells. J Exp Clin Cancer Res 2012; 31: 47.
[19] El Fakhry Y, Alturaihi H, Yacoub D, Liu L, Guo W, Leveillé C, Jung D, Khzam LB, Merhi Y, Wilkins JA, Li H, Mourad W. Functional interaction of CD154 protein with α5β1 integrin is totally independent from its binding to αIIbβ3 integrin and CD40 molecules. J Biol Chem 2012; 287: 18055-18066.
[20] Dormond O, Contreras AG, Meijer E, Datta D, Flynn E, Pal S, Briscoe DM. CD40-induced signaling in human endothelial cells results in mTORC2- and Akt-dependent expression of vascular endothelial growth factor in vitro and in vivo. J Immunol 2008; 181: 8088-8095.
[21] Nakajima T, Hirata M, Shearer T, Azuma M. Mechanism for laser- induced neovascularization in rat choroid: Accumulation of integrin α chain-positive cells and their ligands. Mol Vis 2014; 20: 864-871.
[22] Li R, Chen WC, Pang XQ, Tian WY, Zhang XG. Influence of SCD40l on gastric cancer cell lines. Mol Biol Rep 2011; 38: 5459-5464.
[23] Kawabe T, Matsushima M, Hashimoto N, Imaizumi K, Hasegawa Y. CD40/CD40 ligand interactions in immune responses and pulmonary immunity. Nagoya J Med Sci 2011; 73: 69-78.
[24] Ramello MC, Boari JT, Canale FP, Mena HA, Negrotto S, Gastman B, Gruppi A, Acosta Rodríguez EV, Montes CL. Tumor-induced senescent T cells promote the secretion of pro-inflammatory cytokines and angiogenic factors by human monocytes/macrophages through a mechanism that involves Tim-3 and CD40L. Cell Death Dis 2014; 5: e1507.